

Efficiency corrections for mutually inclusive variables and particle identification effect for mixed-cumulants in heavy-ion collisions

Arghya Chatterjee,^{1,*} Toshihiro Nonaka,^{2,†} Shinichi Esumi,^{2,‡} and Xiaofeng Luo^{1,§}

¹*Key Laboratory of Quark & Lepton Physics (MOE) and Institute of Particle Physics,
Central China Normal University, Wuhan 430079, China*

²*Tomonaga Center for the History of the Universe, University of Tsukuba, Tsukuba, Ibaraki 305, Japan*

Mix-cumulants of conserved charge distributions are sensitive observables to probe properties of the QCD medium and phase transition in heavy-ion collisions. In order to perform a precise measurement, efficiency correction is one of the most important steps. In this paper, we derive the proper efficiency correction formulas for mutually exclusive and inclusive variables. UrQMD model is applied to check the validity of those formulas for different types of correlations. Further, we investigate the effect of the multiplicity loss and contamination arising from the particle identifications. This study provides an important step towards future measurements of mixed-cumulants in relativistic heavy-ion collisions.

I. INTRODUCTION

Heavy-ion collisions at relativistic energies produce matter at extreme conditions of energy density and temperature. This new form of matter consists of deconfined quarks and gluons and is called Quark-Gluon Plasma (QGP). One of the primary aims of heavy-ion collision experiments is to explore the phase structure of the hot dense QCD matter. The QCD phase structure can be expressed as a function of temperature (T) and baryon chemical potential (μ_B) [1]. QCD based model calculations predict that at large μ_B the transition between hadronic matter to QGP is of first order [2, 3]. The end point of the first order phase transition boundary is known as QCD critical point (CP), after which there is no genuine phase transition but a smooth crossover from hadronic to quark-gluon degrees of freedom [4, 5]. One of the main approaches for exploring the QCD phase structure is through measurements of event-by-event fluctuations of conserved quantities, such as net-baryon (B), net-charge (Q) and net-strangeness (S) [6–10]. In a thermodynamic system, r -th order fluctuation ('cumulants') of event-by-event net-multiplicity distributions are related to the r -th order thermodynamic susceptibilities of the corresponding conserved charges that diverge near the critical point [11–14]. Furthermore, those measured cumulants have also been used to extract freeze-out parameters (T and μ_B) by comparing with model calculations from lattice QCD and hadron resonance gas (HRG) [15–19]. Due to the experimental constraints on measuring neutral particle yields, net-proton and net-kaons are used as an experimental proxies of net-baryon and net-strangeness respectively. In the last decade, the STAR and PHENIX experiments at Relativistic Heavy Ion Collider (RHIC) have measured the second, third and fourth order cumulants of net-proton [20–23], net-charge [24, 25] and net-kaon [26] multiplicity distributions over a wide range of collision energies to find non-monotonic energy dependence behaviours as signal to the presence of the CP. Within current statistical uncertainties no distinctive signatures of the CP have been inferred from the net-charge and net-kaon measurements. However, recent measurement of fourth order to second order cumulant ratios of net-proton multiplicity distributions exhibit non-monotonic energy dependence as a function of $\sqrt{s_{NN}}$ [22]. Although, before drawing any strong physics conclusions from event-by-event fluctuation measurements, we need to carefully investigate the different background contributions [27–32].

Recently STAR experiment has reported the first measurement of second-order mixed-cumulants between net-charge, net-proton and net-kaon multiplicity distributions in the first phase of beam energy scan (BES-I) program at RHIC [33]. These mixed-cumulants are related to the off-diagonal thermodynamic susceptibilities that carry the correlation between different conserved charges of QCD [34–40]. The importance of second-order mixed-cumulants was first highlighted in the context of normalized baryon-strangeness susceptibilities ($C_{B,S} = -3\chi_{B,S}^{1,1}/\chi_S^2$) in Ref. [34], which are expected to show a rapid change with the onset of deconfinement. Those quantities can be inquired by measuring the energy dependence ratios of off-diagonal over diagonal cumulants ratios between net-baryon and net-strangeness ($C_{B,S}^{1,1}/C_S^2$). Another research goal comes from the comparisons between the ideal HRG model and lattice QCD calculations. The baryon-charge susceptibility ($\chi_{B,Q}^{1,1}$) shows a significant difference between lattice and ideal HRG calculation above the crossover transition temperature even in at lowest order [41, 42]. A similar difference between lattice and HRG calculation can also be observed in higher-order baryon susceptibilities ((χ_B^4)), which is more statistically challenged in experimental measurement [43]. Similar to diagonal cumulants the mixed-cumulants also

*Electronic address: arghya@mail.ccnu.edu.cn, arghya@rcf.rhic.bnl.gov

†Electronic address: nonaka.toshihiro.ge@u.tsukuba.ac.jp

‡Electronic address: esumi.shinichi.gn@u.tsukuba.ac.jp

§Electronic address: xfluo@ccnu.edu.cn

challenged by the lack of neutral particles detection capability. Measurements of charge-baryon or charge-strangeness mixed-cumulants are less affected by such experimental limitation as the neutral particles does not contribute to such charge correlations, and can be approximated by $C_{Q,B}^{1,1} \approx C_{Q,p}^{1,1}$ and $C_{Q,S}^{1,1} \approx C_{Q,k}^{1,1}$ [39]. On the other hand baryon-strangeness mixed-cumulants cannot be approximated by proton-kaon off-diagonal. However, the relation between those have been studied in Ref. [39, 44].

Recent measurements of second-order mixed-cumulants at RHIC energy range ($\sqrt{s_{NN}} = 7.7\text{-}200$ GeV) shows a good agreement with different model predictions for net proton-kaon off-diagonal correlator ($C_{p,k} = \sigma_{p,k}^{1,1}/\sigma_k^2$). However, the charge-proton ($C_{Q,p} = \sigma_{Q,p}^{1,1}/\sigma_p^2$) and charge-kaon ($C_{Q,k} = \sigma_{Q,k}^{1,1}/\sigma_k^2$) correlator shows a significant deviation from model predicted values. In this work we demonstrate that the deviations observed in charge-proton and charge-kaon correlators are due to the efficiency double counting. We argue that, to correct the effects of efficiency for charge-proton and charge-kaon mixed-cumulants, the particle identification for charge needs to be done with estimating corresponding efficiencies. Though a significant number of charged tracks are missed for particle identification as different detectors used [33]. In this paper, we focus on the 2nd-order mixed-cumulant for two variables to clarify and simplify several important points on the efficiency correction. Although the points also apply for higher-order mixed-cumulants and for more than two variables cases, those extensions should be straightforward and are expected to be investigated in future works.

This paper is organized as follows. In Sec II, cumulants, mixed-cumulants, and their efficiency corrections are introduced. The formulas for the efficiency correction of the 2nd-order mixed-cumulant is discussed for two types of correlations. In Sec. III, we perform numerical analysis using the UrQMD model to check the importance of using appropriate formulas depending on the correlation type. Effects of double-counting will be discussed. The potential effect of the multiplicity loss due to particle identification are investigated. We then summarize our present studies in Sec. IV.

II. EFFICIENCY CORRECTION

A. Cumulants and mixed-cumulants

In statistics, any distribution can be characterized by different order moments or cumulants. The r th-order moment of variable N is defined by the r th order derivative of moment generating function $G(\theta)$:

$$G(\theta) = \sum_N e^{N\theta} P(N) = \langle e^{N\theta} \rangle, \quad (1)$$

$$\langle N^r \rangle = \left. \frac{d^r}{d\theta^r} G(\theta) \right|_{\theta=0}, \quad (2)$$

where $P(N)$ is a probability distribution function, and $\langle \cdot \rangle$ represents an average over events. Cumulants are defined through the cumulant generating function $K(\theta)$:

$$T(\theta) = \ln G(\theta), \quad (3)$$

$$\langle N^r \rangle_c = \left. \frac{d^r}{d\theta^r} T(\theta) \right|_{\theta=0}, \quad (4)$$

where $\langle \cdot \rangle_c$ represents the cumulant of the variable inside the bracket. From Eqs. 1–4, the 1st and 2nd-order cumulants are expressed in terms of moments

$$\langle N \rangle_c = \langle N \rangle, \quad (5)$$

$$\langle N^2 \rangle_c = \langle N^2 \rangle - \langle N \rangle^2, \quad (6)$$

Similarly, the multivariate moments and cumulants are defined by multivariate generating function. In the present study, we focus on the two-variable case, which we call "mixed-" moments or cumalants, where the moment generating function is given by

$$G(\theta_1, \theta_2) = \sum_{N_1, N_2} e^{\theta_1 N_1} e^{\theta_2 N_2} P(N_1, N_2) = \langle e^{\theta_1 N_1} e^{\theta_2 N_2} \rangle, \quad (7)$$

$$\langle N_1^{r_1} N_2^{r_2} \rangle = \left. \frac{\partial^{r_1}}{\partial \theta_1^{r_1}} \frac{\partial^{r_2}}{\partial \theta_2^{r_2}} G(\theta_1, \theta_2) \right|_{\theta_1=\theta_2=0}. \quad (8)$$

Mixed-cumulants are then defined as:

$$T(\theta_1, \theta_2) = \ln G(\theta_1, \theta_2), \quad (9)$$

$$\langle N_1^{r_1} N_2^{r_2} \rangle_c = \left. \frac{\partial^{r_1}}{\partial \theta_1^{r_1}} \frac{\partial^{r_2}}{\partial \theta_2^{r_2}} T(\theta_1, \theta_2) \right|_{\theta_1=\theta_2=0}. \quad (10)$$

From Eqs. 7–10 we obtain the 2nd-order mixed-cumulant in terms of moments and mixed-moments:

$$\langle N_1 N_2 \rangle_c = \langle N_1 N_2 \rangle - \langle N_1 \rangle \langle N_2 \rangle. \quad (11)$$

B. Binomial model

The particle detection efficiency of each detector is always limited. The event-by-event particle multiplicity distributions are convoluted due to this finite detector efficiency. The efficiency correction needs to be done to recover the true multiplicity distribution. It is well established that detection efficiency is well estimated by binomial efficiency response function [45, 46]. The mean value (first-order moment/cumulant) can be easily reconstructed by dividing by the binomial efficiency response, but its influence on higher-order cumulants are complicated and depends on the probability distribution of efficiency [47–49]. Throughout this paper, we focus on a simple assumption of the binomial distribution given by

$$\tilde{P}(n) = \sum_N P(N) B_{\varepsilon, N}(n), \quad (12)$$

$$B_{\varepsilon, N}(n) = \frac{N!}{n!(N-n)!} \varepsilon^n (1-\varepsilon)^{N-n}, \quad (13)$$

where ε represents the efficiency, N and n are generated and measured particles, respectively. Under this situation, correction formulas can be derived in straightforward manner as discussed in the literature [50–57]. The efficiency correction for the 2nd-order mixed-cumulant is given by [56, 57]

$$\langle\langle K_{(x)} K_{(y)} \rangle\rangle_c = \langle\kappa_{(1,0,1)} \kappa_{(0,1,1)}\rangle_c + \langle\kappa_{(1,1,1)}\rangle_c - \langle\kappa_{(1,1,2)}\rangle_c, \quad (14)$$

with

$$K_{(x)} = \sum_i^M x_i n_i, \quad K_{(y)} = \sum_i^M y_i n_i, \quad (15)$$

$$\kappa(r, s, t) = \sum_{i=1}^M \frac{x_i^r y_i^s}{\varepsilon_i^t} n_i. \quad (16)$$

where $\langle\langle \cdot \rangle\rangle$ represents the efficiency correction, M is the number of efficiency bins, n_i is the number of particles, ε_i is the efficiency, x_i and y_i are the electric charge of the particles at the i th efficiency bin. It is noteworthy that Eqs. 15 and 16 can be rewritten in track-by-track notations as

$$K_{(x)} = \sum_j^{n^{\text{tot}}} x_j, \quad K_{(y)} = \sum_j^{n^{\text{tot}}} y_j, \quad (17)$$

$$\kappa(r, s, t) = \sum_{j=1}^{n^{\text{tot}}} \frac{x_j^r y_j^s}{\varepsilon_j^t}, \quad (18)$$

where $n_{\text{tot}} = \sum_i^M n_i$ is the number of measured particles in one event, and the other variables are now track-wise with j running over the particles in the summation.

In the rest of this section, we consider two efficiency bins for simplicity. Particles for each bin have the same efficiency value, ε_1 and ε_2 , respectively. The number of particles will be denoted by n_1 and n_2 .

C. Mutually exclusive variable

Let's consider the correlation between two mutually exclusive variable. From Eq. 10 the mixed-cumulant of generated particles are expanded in terms of moments as

$$\langle N_1 N_2 \rangle_c = \langle N_1 N_2 \rangle - \langle N_1 \rangle \langle N_2 \rangle. \quad (19)$$

To perform the efficiency correction with respect to measured particles, we suppose

$$x = (x_1, x_2) = (1, 0), \quad (20)$$

$$y = (y_1, y_2) = (0, 1), \quad (21)$$

to consider $\langle\langle K_{(x)} K_{(y)} \rangle\rangle_c$ with $K_{(x)} = n_1$ and $K_{(y)} = n_2$. From Eq. 14 we get

$$\langle\langle K_{(1,0)} K_{(0,1)} \rangle\rangle_c = \langle\kappa(1, 0, 1) \kappa(0, 1, 1)\rangle_c + \langle\kappa(1, 1, 1)\rangle_c - \langle\kappa(1, 1, 2)\rangle_c \quad (22)$$

$$= \left\langle \frac{n_1}{\varepsilon_1} \frac{n_2}{\varepsilon_2} \right\rangle_c \quad (23)$$

$$= \frac{1}{\varepsilon_1 \varepsilon_2} \langle n_1 n_2 \rangle - \frac{1}{\varepsilon_1 \varepsilon_2} \langle n_1 \rangle \langle n_2 \rangle, \quad (24)$$

This is the basic formula of the efficiency correction for the 2nd-order mixed-cumulant for two variables.

D. Mutually inclusive variables

1. Problem

Next, we consider the correlation between N_1 and $N_1 + N_2$, i.e, when the two variables are not mutually exclusive. It is clear we have the self-correlation of N_1 . The 2nd-order mixed-cumulant can be expanded as

$$\langle N_1(N_1 + N_2) \rangle_c = \langle N_1 N_2 \rangle - \langle N_1 \rangle \langle N_2 \rangle + \langle N_1^2 \rangle - \langle N_1 \rangle^2, \quad (25)$$

where the last two terms represent the variance (2nd-order cumulant, $\langle N_1^2 \rangle_c$). If we employ Eq. 24 for the efficiency correction, we can just replace n_1 to $n_1 + n_2$ as

$$\langle\langle K_{(1,0)} K_{(0,1)} \rangle\rangle_c = \frac{1}{\varepsilon_1 \varepsilon_2} \langle n_1(n_1 + n_2) \rangle - \frac{1}{\varepsilon_1 \varepsilon_2'} \langle n_1 \rangle \langle n_1 + n_2 \rangle, \quad (26)$$

$$= \frac{1}{\varepsilon_1 \varepsilon_2} \langle n_1 n_2 \rangle - \frac{1}{\varepsilon_1 \varepsilon_2'} \langle n_1 \rangle \langle n_2 \rangle + \frac{1}{\varepsilon_1 \varepsilon_2'} \langle n_1^2 \rangle - \frac{1}{\varepsilon_1 \varepsilon_2'} \langle n_1 \rangle^2, \quad (27)$$

with ε_2' being the averaged efficiency for N_1 and N_2 given by

$$\varepsilon_2' = \frac{\langle N_1 \rangle \varepsilon_1 + \langle N_2 \rangle \varepsilon_2}{\langle N_1 \rangle + \langle N_2 \rangle}, \quad (28)$$

which is not an appropriate efficiency corrected expression for mutually inclusive variables. To confirm this, let us suppose two independent variable N_1 and N_2 , and they follow Poisson distribution with $\langle N_1 \rangle = 4$ and $\langle N_2 \rangle = 6$. It is known that the relation $\langle N^r \rangle_c = \langle N \rangle_c^r$ holds for Poisson distributions, thus $\langle N^2 \rangle_c = \langle N^2 \rangle - \langle N \rangle^2$, which leads to $\langle N_1(N_1 + N_2) \rangle_c = 4$ from Eq. 25. The relation $\langle N_1 N_2 \rangle = \langle N_1 \rangle \langle N_2 \rangle$ was used for independent variables. We then consider the efficiency correction for $\varepsilon_1 = 0.5$ and $\varepsilon_2 = 0.4$. One finds

$$\varepsilon_2' = 0.44, \quad \langle n_1 \rangle = 2, \quad \langle n_2 \rangle = 2.4, \quad (29)$$

$$\langle n_1^2 \rangle_c = \langle n_1^2 \rangle - \langle n_1 \rangle^2 = 2, \quad (30)$$

$$\langle n_1 n_2 \rangle = \langle n_1 \rangle \langle n_2 \rangle, \quad (31)$$

which leads to the efficiency corrected mixed-cumulant value

$$\langle\langle K_{(1,0)} K_{(0,1)} \rangle\rangle_c = 4.55. \quad (32)$$

Thus Eq. 24 is not valid for the self correlated or mutually inclusive case.

2. Solution

The solution is to use the appropriate indices for x and y in Eqs. 16 and 15. To consider $\langle\langle K_{(x)} K_{(y)} \rangle\rangle_c$ with $K_{(x)} = n_1$ and $K_{(y)} = n_1 + n_2$, the indices should have been

$$x = (x_1, x_2) = (1, 0), \quad (33)$$

$$y = (y_1, y_2) = (1, 1), \quad (34)$$

thus

$$\langle\langle K_{(1,0)} K_{(1,1)} \rangle\rangle_c = \langle \kappa(1, 0, 1) \kappa(0, 1, 1) \rangle_c + \langle \kappa(1, 1, 1) \rangle_c - \langle \kappa(1, 1, 2) \rangle_c \quad (35)$$

$$= \frac{1}{\varepsilon_1 \varepsilon_2} \langle n_1 n_2 \rangle - \frac{1}{\varepsilon_1 \varepsilon_2} \langle n_1 \rangle \langle n_2 \rangle + \frac{1}{\varepsilon_1^2} \langle n_1^2 \rangle - \frac{1}{\varepsilon_1^2} \langle n_1 \rangle^2 + \frac{1}{\varepsilon_1} \langle n_1 \rangle - \frac{1}{\varepsilon_1^2} \langle n_1 \rangle, \quad (36)$$

where we find additional two terms compared with Eq. 27. It is found that the last 4 terms in Eq. 36 represents the efficiency correction of the variance (2nd-order cumulant), $\langle\langle K_{(x)}^2 \rangle\rangle_c$, which corresponds to the last two terms in Eq. 25 [71]. This indicates that the term of variance has to be taken into account correctly for the mutually inclusive variable case, which cannot be handled by Eq. 24.

Let us summarize this section as follows. The formula of efficiency correction for the 2nd-order mixed-cumulant was fully expanded for two cases: one is for two mutually exclusive variables, and the other case assumes that one variable is a subset of other, to consider the self-correlation, as shown in Eqs. 24 and 36. The both were found to be incompatible each other. One needs to obtain the proper correction formulas by substituting appropriate indices into Eqs. 14–16. This implies that one has to handle the efficiency values properly for each variable without averaging them, especially when considering the self-correlation. It should be noted that the risk of using the averaged efficiency had been pointed out in Ref. [56] for higher-order cumulants of single-variable. The efficiency bins always need to be carefully handled. The track-by-track efficiency through identified particle approach shown in Eqs. 17 and 18 would be a better way to handle all possible variations of efficiencies [57]. On the other hand, the particle identification needs to be applied in order to determine the efficiencies for different particle species, which removes not a small amount of particles depending on the overlapping area of the variables for the particle identification. This effect will be studied by numerical simulations in the next section [24, 58].

III. NUMERICAL ANALYSIS IN URQMD MODEL

A. Closure test using UrQMD model

In order to validate the discussion from the previous section, we have analysed the second-order mixed cumulants from the UrQMD event generator at $\sqrt{s_{NN}} = 200$ GeV. The UrQMD is a microscopic transport model, where the space-time evolution of the fireball is considered in terms of excitation of color strings that fragment further into hadrons, the co-variant propagation of hadrons and resonances that undergo scatterings, and finally the decay of all the resonances [59, 60]. Collision energy dependence baryon stopping phenomenon dynamically incorporated in the UrQMD model. UrQMD model has been quite successful and widely used towards heavy-ion phenomenology [60, 61]. Previously, this model has been used to study several fluctuation observable and cumulants [27, 39, 62–66]. More information about the UrQMD model can be found in the reference [59, 60]. In this study, we have used around million events for Au+Au collisions at $\sqrt{s_{NN}} = 200$ GeV to study the efficiency correction effect on mixed cumulants. The results are presented for 9 different centrality bins represented by the average number of participant nucleons ($\langle N_{part} \rangle$). In this study, we have used the same kinematic acceptance $|\eta| < 0.5$ and $0.4 < p_T < 1.6$ GeV/c as STAR data [33]. The collision centrality is defined using RefMult2 (charged particle multiplicity with in the pseudorapidity range $0.5 < |\eta| < 1.0$) to reduce the centrality auto-correlation effect [27, 28]. Figure 1 shows the centrality dependence second-order mixed-cumulants of net-charge, net-proton and net-kaon multiplicity distributions from the UrQMD model. The black solid points represent the 'true' mixed-cumulants values. To introduce the detector efficiency effect we passed the binomial filter to the counted particles number in each event. We used two p_T -bin and positive-negative separate efficiencies similar to real data analysis. Then we estimate the mixed-cumulants with filtered particle numbers represented by red square points, which are analogous to efficiency uncorrected values.

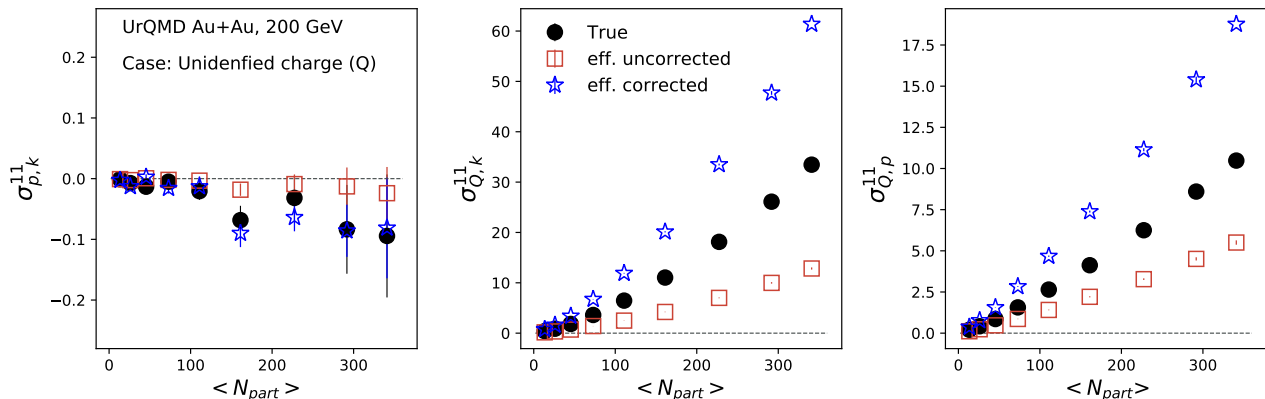


FIG. 1: (Color online) Centrality dependence second-order mixed-cumulants of net-charge ($Q = N_{Q^+} - N_{Q^-}$), net-proton ($p = N_p - N_{\bar{p}}$) and net-kaon ($k = N_{k^+} - N_{k^-}$) multiplicity for Au+Au collisions at 200 GeV using UrQMD model. The efficiency correction are done assuming variables are mutually exclusive (Eq. 24).

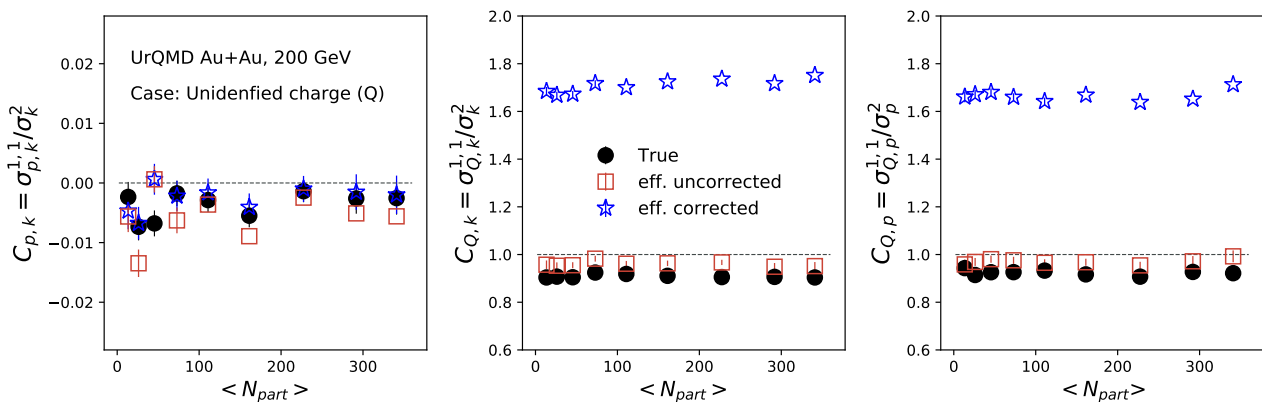


FIG. 2: (Color online) Centrality dependence second-order off-diagonal to diagonal cumulants ratios for Au+Au collisions at 200 GeV using UrQMD model. The efficiency correction are done assuming variables are mutually exclusive.

In the next step, we correct the efficiency using input efficiency values. In this case, we used unidentified charged

particles for net-charge (Q) and applied Eq. 24 as used in STAR measurement. The p - k mixed cumulant 'true' value can be reproduced using this method as they are mutually exclusive variables. However, the efficiency correction for Q - p and Q - k fails to reproduce the 'true' values as we discussed in Sec. II. We end up with a higher value for unidentified charge correlators. This leads to a higher value in cumulant ratios $C_{Q,k} = \sigma_{Q,k}/\sigma_k^2$ and $C_{Q,p} = \sigma_{Q,p}/\sigma_p^2$ from 'true' values as seen in Fig. 2. This shows that Eq. 24 is not valid for overlap or mutually exclusive variables. However, for mutually inclusive variables (like protons-kaons) there is no issue. As we discussed before, to correct the mixed cumulant for mutually inclusive variables we need to use Eq. 36. To apply Eq. 36 for Q - k and Q - p mixed cumulants it is necessary to identify the charged particles with their efficiencies. In Fig. 36, we consider only identified charged particles ($Q = \pi + k + p$). Then Eq. 36 becomes

$$\begin{aligned} \langle\langle N_Q N_k \rangle\rangle_c &= \langle\langle (N_\pi + N_p + N_k) N_k \rangle\rangle_c \\ &= \frac{1}{\varepsilon_1 \varepsilon_3} \langle N_\pi N_k \rangle - \frac{1}{\varepsilon_1 \varepsilon_3} \langle N_\pi \rangle \langle N_k \rangle + \frac{1}{\varepsilon_2 \varepsilon_3} \langle N_p N_k \rangle - \frac{1}{\varepsilon_2 \varepsilon_3} \langle N_p \rangle \langle N_k \rangle + \frac{1}{\varepsilon_3^2} \langle N_k^2 \rangle - \frac{1}{\varepsilon_3^2} \langle N_k \rangle^2 \\ &\quad + \frac{1}{\varepsilon_3} \langle N_k \rangle - \frac{1}{\varepsilon_3^2} \langle N_k \rangle, \end{aligned} \quad (37)$$

where ε_1 , ε_2 and ε_3 are the efficiencies for pions, kaons and protons respectively. Now we can reproduce the 'true' values as shown in Figs. 3 and 4.

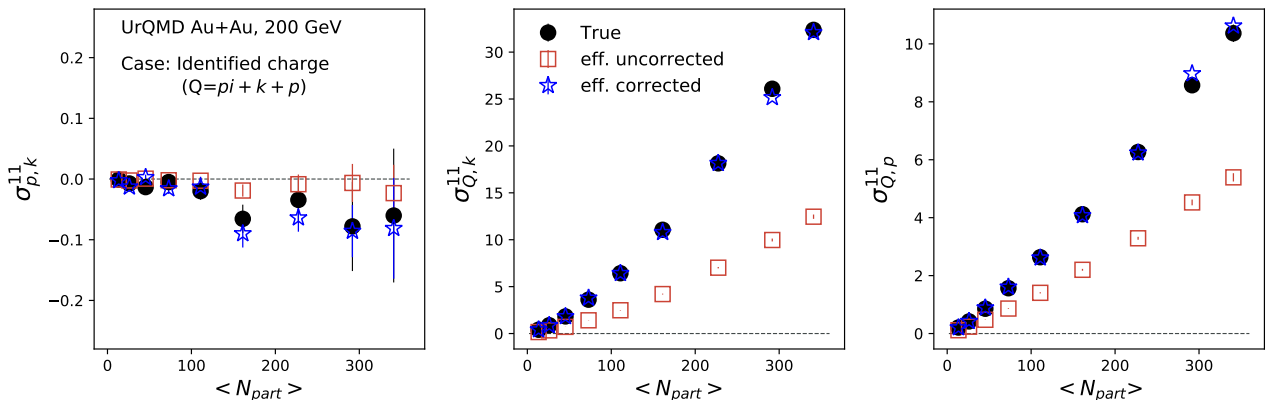


FIG. 3: (Color online) Centrality dependence second-order mixed-cumulants of identified net-charge ($Q = (N_{\pi^+} + N_{k^+} + N_p) - (N_{\pi^-} + N_{k^-} + N_{\bar{p}})$), net-proton ($p = N_p - N_{\bar{p}}$) and net-kaon ($k = N_{k^+} - N_{k^-}$) multiplicity for Au+Au collisions at 200 GeV using UrQMD model. The efficiency correction are done assuming variables are mutually inclusive (Eq. 36).

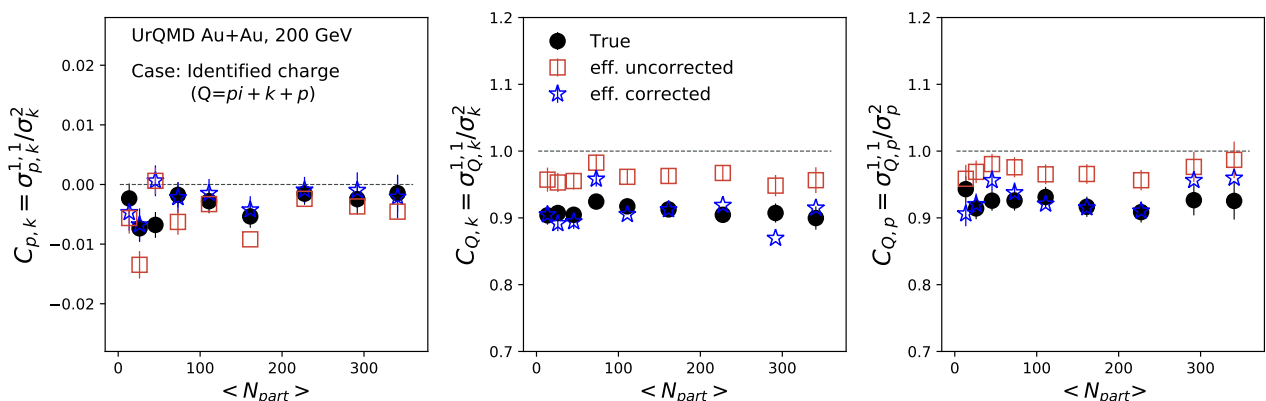


FIG. 4: (Color online) Centrality dependence second-order off-diagonal to diagonal cumulants ratios of identified charged particles for Au+Au collisions at 200 GeV using UrQMD model. The efficiency correction are done assuming variables are mutually inclusive.

However, due to particle identification with good purity we may lose some pions, protons and kaons. We also studied the effect of those tracks for mixed cumulants using UrQMD simulations. Charged particle identification is done through ionization energy loss inside the Time Projection Chamber (TPC) detector subsystem. We mimic the ionization energy loss curve in UrQMD simulation using STAR TPC resolution. Figure 5(a) shows the measured

dE/dx distribution after passing the UrQMD input through TPC simulation. The measured values of dE/dx are compared to the expected theoretical values which is an extension of the Bethe-Bloch formula [67] (shown as dashed lines in Fig. 5(a)). To identify particles X, a quantity $n\sigma_X$ is defined as

$$n\sigma_X = \frac{1}{R} \ln \frac{[dE/dx]_{obs}}{[dE/dx]_{th,X}}, \quad (38)$$

where $[dE/dx]_{obs}$ is the energy loss in UrQMD simulation and $[dE/dx]_{th,X}$ is the corresponding theoretical value for particle species X. R is the dE/dx resolution and we used $R = 7.5\%$ with in our analysis range. Figure 5(b) shows the $n\sigma$ distributions of $p(\bar{p})$, π^\pm and k^\pm . Usually $n\sigma_p < 2$ are used for $p(\bar{p})$ selection. Similarly, $n\sigma_\pi < 2$ and $n\sigma_k < 2$ are used for pions and kaons selection respectively. However, from Fig. 5(a) we can see that at high momentum the dE/dx bands for different particles are overlapped. We have also used the 2σ -rejection cut to improve the purity.

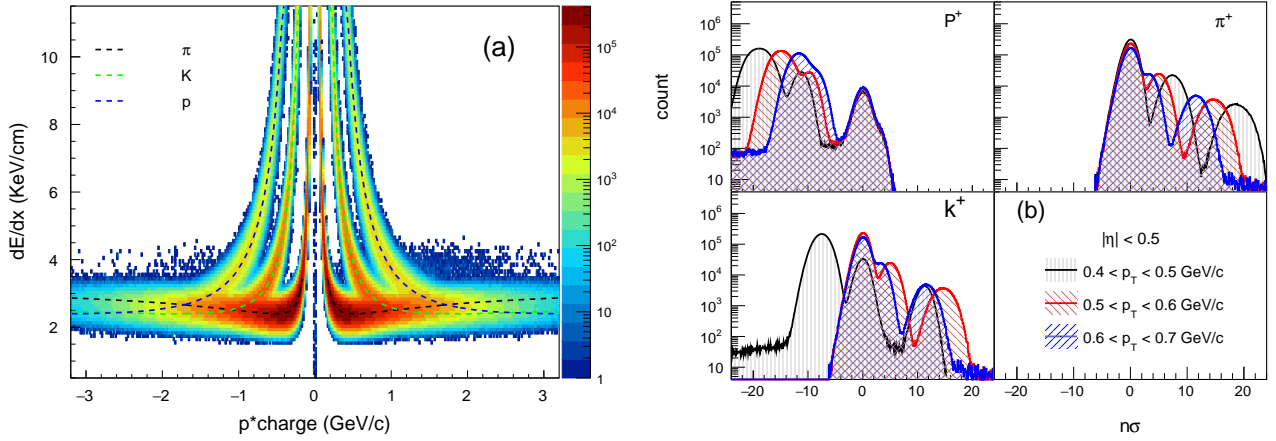


FIG. 5: (Color online) (a) dE/dx from UrQMD simulations plotted against charge \times momentum of individual particles for Au+Au collisions at $\sqrt{s_{NN}} = 200$ GeV. (b) $n\sigma$ distributions of protons, pions and kaons.

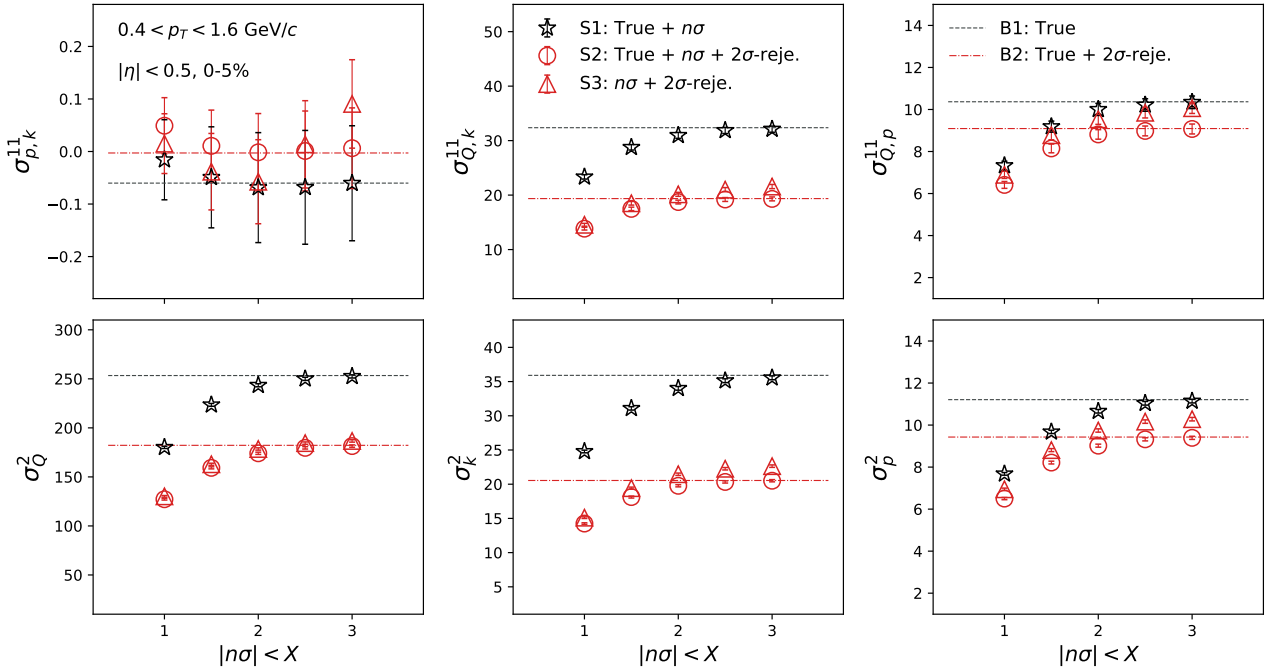


FIG. 6: (Color online) $n\sigma$ acceptance dependence second-order off-diagonal and diagonal cumulants for Au+Au collisions at 200 GeV using UrQMD model.

For	Legend	Particle Code	$n\sigma$	2σ -rejection	Baseline
Signal	S1	Used	Applied	N/A	B1
	S2	Used	Applied	Applied	B2
	S3	N/A	Applied	Applied	B2
Baseline	B1	Used	N/A	N/A	N/A
	B2	Used	N/A	Applied	N/A

TABLE I: This table describes which information is used to select the particles for mixed-cumulant calculations in Fig. 6, in terms of the particle species code given by UrQMD, $n\sigma$ and 2σ -rejection cuts. Corresponding legends in Fig. 6 are shown in the second left row.

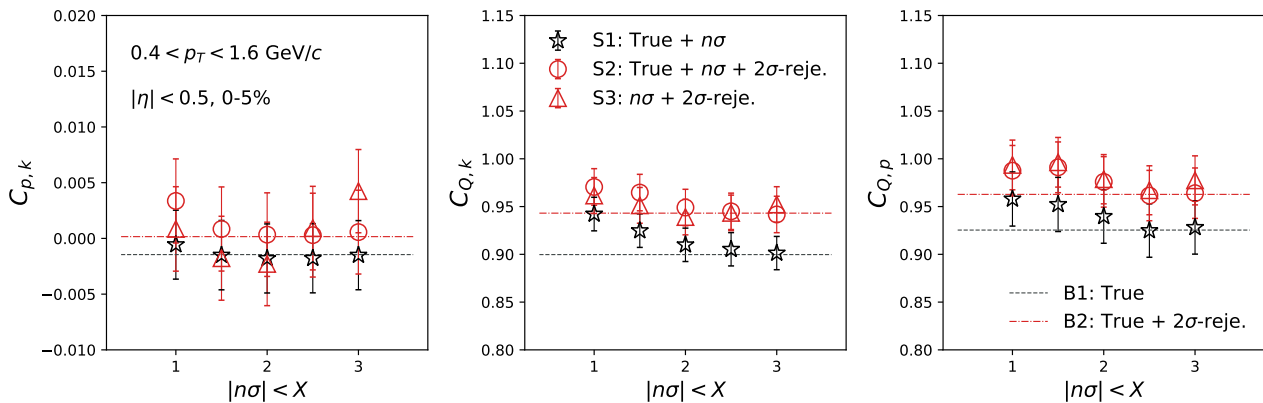


FIG. 7: (Color online) $n\sigma$ acceptance dependence second-order off-diagonal over diagonal cumulants ratios for Au+Au collisions at 200 GeV using UrQMD model.

Figure 6 shows mixed-cumulants as a function of $n\sigma$ cut for three cases as follows (see Tab. I):

S1 : Information of the particle species is given by UrQMD. The $n\sigma$ cut is applied.

S2 : Information of the particle species is given by UrQMD. Both $n\sigma$ and 2σ -rejection cuts are applied.

S3 : Particles are identified by both $n\sigma$ and 2σ -rejection cuts. This is the only possible cut in the experimental data analysis.

We note that "Q" is defined as the summation of identified π , K , and p . The " 2σ -rejection cut" represents to require $n\sigma_K > 2.0$ and $n\sigma_\pi > 2.0$ for proton identification, $n\sigma_p < -2.0$ and $n\sigma_\pi > 2.0$ for kaon identification, and $n\sigma_K < -2.0$ and $n\sigma_p < -2.0$ for pion identification, respectively. Further, two baselines are calculated with following conditions, which are independent on $n\sigma$ cut:

B1 : Information of the particle species is given by UrQMD.

B2 : Information of the particle species is given by UrQMD. The 2σ -rejection cut is applied.

The difference between two baselines is due to the particle multiplicity. There are more particles for B1 than B2 since the 2σ -rejection cut is applied to the latter case. Depending on whether the 2σ -rejection cut is applied, one can compare S1 to B1, while S2 and S3 needs be compared to B2, respectively. The descriptions of Fig. 6 are summarized in Tab. I.

It is found that the values of mixed-cumulants are close to corresponding baselines with a loose $n\sigma$ cut, and decreases with tightening the $n\sigma$ cut. As one can see in Eq. 19, the mixed-cumulant for mutually inclusive case consists of second-order cumulant as well as second-order mixed-cumulants. It is well known that the former one has a trivial volume dependence [68], which can be also confirmed from the lower panels in Fig. 6 for the second-order cumulants. In Fig. 6, therefore, only $\sigma_{p,k}^{11}$ is independent on the $n\sigma$ cut. The difference between S2 and S3 would indicate the effect of contamination. It can be confirmed from the fact that the difference becomes small with tightening the $n\sigma$ cut, in addition to the 2σ -rejection cut. As a result we observed larger values of $\sigma_{Q,k}^{11}$ and $\sigma_{Q,p}^{11}$ for S3 compare to S2.

In order to cancel the trivial volume dependence, the normalized mixed-cumulants are also calculated in Fig. 7 as a function of the $n\sigma$ cut. All results for S1, S2, and S3 are found to be consistent with corresponding baselines within uncertainties. This is because the probability of the contamination has been significantly suppressed by the 2σ -rejection cut. To confirm this normalized mixed-cumulants with only the $n\sigma$ cut are calculated, where the significant deviations are observed from the corresponding baseline due to contamination. It should be noted that the $n\sigma$ dependence of mixed-cumulants and normalized mixed-cumulants also depend on how the intrinsic correlations between two variables change with respect to the $n\sigma$ cut. In the current simulation, energy loss of the particles are randomly smeared to

implement the resolution of the detectors. Therefore, the correlation terms (the first term on the right hand side in Eqs. 19 and 25) are considered not to get affected by the $n\sigma$ cut. Experimentally, however, this effect needs to be carefully studied by changing the criteria for particle identifications.

IV. SUMMARY

In this study, we discuss the efficiency correction problem for mixed-cumulants. This study provides a comprehensive extension of the binomial efficiency correction formula for second-order mixed cumulants into two different cases: one is for mutually exclusive variables and the other for mutually inclusive variables. We conclude that different efficiency correction formulas need to be applied for mixed-cumulants depending on the type of variable pairs. To apply binomial efficiency correction for Q - k and Q - p mixed cumulants it is necessary to identify the charged particles with their corresponding efficiencies.

It should be noted that the efficiency correction for mixed-cumulants in the case of mutually inclusive variable has been discussed by Ref. [69]. In the proposed formulas, two different levels of efficiencies are implemented for each variable like N_Q and N_p in the case of $\sigma_{Q,p}^{11}$. The tracking efficiency is applied for N_Q , while the proton identification efficiency is applied on top of the tracking efficiency for N_p . The method has the advantage that we can keep charged particles as much as possible without identifying each particle species contained in N_Q . This implies that the averaged efficiencies for pions, kaons, and protons are used for N_Q . However, we must remember that using the averaged efficiency does not give the true answer, which depends on underlying probability distribution of the number of particles and the difference in efficiency between particle species [56]. It is also important to note that the identity method would be useful for the measurements of mixed-cumulants [70], which enables us to measure the fluctuations without the multiplicity loss due to particle identification. It would be nice if we have the new ideas to deal with the two-step efficiency based on the identity method [70].

At this stage, identification of each particle specie and implement the appropriate efficiency accordingly is the simplest approach. Therefore, we further investigate the effect of the loss of the multiplicity due to particle identifications using numerical simulations. In the case of mutually inclusive variable, the mixed-cumulants exhibit a monotonic decrease as the cut value of particle identification tightens. This can be explained by a trivial volume dependence. On the other hand, the normalized mixed-cumulants are found to be independent on the cut value for the particle identification. This is because the intrinsic correlations between different particle species are assumed to be independent on the variables of the particle identification, which could not be the case in real experiments. Therefore, it is recommended to check the effect by changing the criteria for the particle identifications. This work provides important reference for future measurements of mixed-cumulants in relativistic heavy-ion collisions.

V. ACKNOWLEDGEMENT

We thank Volker Koch, Masakiyo Kitazawa, Nihar Rajan Sahoo, Prithwish Tribedy, Volodymyr Vovchenko, Tapan Nayak and Nu Xu for stimulating discussions. This work is supported by the National Key Research and Development Program of China (Grant No. 2020YFE0202002 and 2018YFE0205201), the National Natural Science Foundation of China (Grant No. 11828501, 11890711 and 11861131009), Ito Science Foundation and JSPS KAKENHI Grant No. 25105504, 19H05598.

-
- [1] K. Rajagopal, Nucl. Phys. **A661**, 150 (1999), hep-ph/9908360.
 - [2] M. A. Stephanov, PoS **LAT2006**, 024 (2006), hep-lat/0701002.
 - [3] E. S. Bowman and J. I. Kapusta, Phys. Rev. **C79**, 015202 (2009), 0810.0042.
 - [4] Y. Aoki, G. Endrodi, Z. Fodor, S. D. Katz, and K. K. Szabo, Nature **443**, 675 (2006), hep-lat/0611014.
 - [5] S. Gupta, X. Luo, B. Mohanty, H. G. Ritter, and N. Xu, Science **332**, 1525 (2011), 1105.3934.
 - [6] M. A. Stephanov, K. Rajagopal, and E. V. Shuryak, Phys. Rev. Lett. **81**, 4816 (1998), hep-ph/9806219.
 - [7] A. Bzdak, S. Esumi, V. Koch, J. Liao, M. Stephanov, and N. Xu, Phys. Rept. **853**, 1 (2020), 1906.00936.
 - [8] X. Luo and N. Xu, Nucl. Sci. Tech. **28**, 112 (2017), 1701.02105.
 - [9] S. Chatterjee and K. A. Mohan, Phys. Rev. D **86**, 114021 (2012), 1201.3352.
 - [10] P. Garg, D. Mishra, P. Netrakanti, B. Mohanty, A. Mohanty, B. Singh, and N. Xu, Phys. Lett. B **726**, 691 (2013), 1304.7133.
 - [11] M. A. Stephanov, Phys. Rev. Lett. **102**, 032301 (2009), 0809.3450.
 - [12] M. Cheng et al., Phys. Rev. **D79**, 074505 (2009), 0811.1006.
 - [13] M. Asakawa, S. Ejiri, and M. Kitazawa, Phys. Rev. Lett. **103**, 262301 (2009), 0904.2089.
 - [14] M. A. Stephanov, Phys. Rev. Lett. **107**, 052301 (2011), 1104.1627.
 - [15] A. Bazavov et al., Phys. Rev. Lett. **109**, 192302 (2012).
 - [16] S. Borsanyi, Z. Fodor, S. D. Katz, S. Krieg, C. Ratti, and K. K. Szabo, Phys. Rev. Lett. **111**, 062005 (2013).
 - [17] P. Alba, W. Alberico, R. Bellwied, M. Bluhm, V. Mantovani Sarti, M. Nahrgang, and C. Ratti, Phys. Lett. **B738**, 305 (2014).
 - [18] F. A. Flor, G. Olinger, and R. Bellwied (2020), 2009.14781.

- [19] S. Gupta, D. Mallick, D. K. Mishra, B. Mohanty, and N. Xu (2020), 2004.04681.
- [20] M. M. Aggarwal et al. (STAR), Phys. Rev. Lett. **105**, 022302 (2010), 1004.4959.
- [21] L. Adamczyk et al. (STAR), Phys. Rev. Lett. **112**, 032302 (2014), 1309.5681.
- [22] J. Adam et al. (STAR), Phys. Rev. Lett. **126**, 092301 (2021), 2001.02852.
- [23] M. Abdallah et al. (STAR) (2021), 2101.12413.
- [24] L. Adamczyk et al. (STAR), Phys. Rev. Lett. **113**, 092301 (2014), 1402.1558.
- [25] A. Adare et al. (PHENIX), Phys. Rev. **C93**, 011901 (2016), 1506.07834.
- [26] L. Adamczyk et al. (STAR), Phys. Lett. B **785**, 551 (2018), 1709.00773.
- [27] X. Luo, J. Xu, B. Mohanty, and N. Xu, J. Phys. **G40**, 105104 (2013), 1302.2332.
- [28] A. Chatterjee, Y. Zhang, J. Zeng, N. R. Sahoo, and X. Luo, Phys. Rev. C **101**, 034902 (2020), 1910.08004.
- [29] Y. Zhang, S. He, H. Liu, Z. Yang, and X. Luo, Phys. Rev. C **101**, 034909 (2020), 1905.01095.
- [30] G. D. Westfall, Phys. Rev. **C92**, 024902 (2015), 1412.5988.
- [31] M. Zhou and J. Jia, Phys. Rev. **C98**, 044903 (2018), 1803.01812.
- [32] A. Chatterjee, Y. Zhang, H. Liu, R. Wang, S. He, and X. Luo (2020), 2009.03755.
- [33] J. Adam et al. (STAR), Phys. Rev. **C100**, 014902 (2019), 1903.05370.
- [34] V. Koch, A. Majumder, and J. Randrup, Phys. Rev. Lett. **95**, 182301 (2005), nucl-th/0505052.
- [35] R. Gavai and S. Gupta, Phys. Rev. D **73**, 014004 (2006), hep-lat/0510044.
- [36] A. Majumder and B. Muller, Phys. Rev. C **74**, 054901 (2006), nucl-th/0605079.
- [37] M. Bluhm and B. Kampfer, Phys. Rev. D **77**, 114016 (2008), 0801.4147.
- [38] H. T. Ding, S. Mukherjee, H. Ohno, P. Petreczky, and H. P. Schadler, Phys. Rev. D **92**, 074043 (2015), 1507.06637.
- [39] A. Chatterjee, S. Chatterjee, T. K. Nayak, and N. R. Sahoo, J. Phys. **G43**, 125103 (2016), 1606.09573.
- [40] R. Bellwied, S. Borsanyi, Z. Fodor, J. N. Guenther, J. Noronha-Hostler, P. Parotto, A. Pasztor, C. Ratti, and J. M. Stafford, Phys. Rev. D **101**, 034506 (2020), 1910.14592.
- [41] A. Bazavov et al. (HotQCD), Phys. Rev. D **86**, 034509 (2012), 1203.0784.
- [42] V. Vovchenko, M. I. Gorenstein, and H. Stoecker, Phys. Rev. Lett. **118**, 182301 (2017), 1609.03975.
- [43] F. Karsch, Nucl. Phys. A **967**, 461 (2017), 1706.01620.
- [44] Z. Yang, X. Luo, and B. Mohanty, Phys. Rev. C **95**, 014914 (2017), 1610.07580.
- [45] A. Bzdak and V. Koch, Phys. Rev. C **86**, 044904 (2012), 1206.4286.
- [46] A. Bzdak and V. Koch, Phys. Rev. C **91**, 027901 (2015), 1312.4574.
- [47] A. Bzdak, R. Holzmann, and V. Koch, Phys. Rev. **C94**, 064907 (2016), 1603.09057.
- [48] T. Nonaka, M. Kitazawa, and S. Esumi, Nucl. Instrum. Meth. **A906**, 10 (2018), 1805.00279.
- [49] S. Esumi, K. Nakagawa, and T. Nonaka, Nucl. Instrum. Meth. A **987**, 164802 (2021), 2002.11253.
- [50] A. Bialas and R. B. Peschanski, Nucl. Phys. **B273**, 703 (1986).
- [51] M. Kitazawa and M. Asakawa, Phys. Rev. **C86**, 024904 (2012), [Erratum: Phys. Rev.C86,069902(2012)], 1205.3292.
- [52] A. Bzdak and V. Koch, Phys. Rev. **C86**, 044904 (2012), 1206.4286.
- [53] A. Bzdak and V. Koch, Phys. Rev. **C91**, 027901 (2015), 1312.4574.
- [54] X. Luo, Phys. Rev. **C91**, 034907 (2015), 1410.3914.
- [55] M. Kitazawa, Phys. Rev. **C93**, 044911 (2016), 1602.01234.
- [56] T. Nonaka, M. Kitazawa, and S. Esumi, Phys. Rev. C **95**, 064912 (2017), [Erratum: Phys.Rev.C 103, 029901 (2021)], 1702.07106.
- [57] X. Luo and T. Nonaka, Phys. Rev. C **99**, 044917 (2019), 1812.10303.
- [58] M. Shao, O. Y. Barannikova, X. Dong, Y. Fisyak, L. Ruan, P. Sorensen, and Z. Xu, Nucl. Instrum. Meth. A **558**, 419 (2006), nucl-ex/0505026.
- [59] S. A. Bass et al., Prog. Part. Nucl. Phys. **41**, 255 (1998), [Prog. Part. Nucl. Phys.41,225(1998)], nucl-th/9803035.
- [60] M. Bleicher et al., J. Phys. **G25**, 1859 (1999), hep-ph/9909407.
- [61] M. Bleicher, M. Belkacem, C. Ernst, H. Weber, L. Gerland, C. Spieles, S. A. Bass, H. Stoecker, and W. Greiner, Phys. Lett. **B435**, 9 (1998), hep-ph/9803345.
- [62] M. Bleicher, S. Jeon, and V. Koch, Phys. Rev. **C62**, 061902 (2000), hep-ph/0006201.
- [63] S. Haussler, H. Stoecker, and M. Bleicher, Phys. Rev. **C73**, 021901 (2006), hep-ph/0507189.
- [64] J. Xu, S. Yu, F. Liu, and X. Luo, Phys. Rev. **C94**, 024901 (2016), 1606.03900.
- [65] S. He and X. Luo, Phys. Lett. **B774**, 623 (2017), 1704.00423.
- [66] M. Mukherjee, S. Basu, A. Chatterjee, S. Chatterjee, S. P. Adhya, S. Thakur, and T. K. Nayak, Phys. Lett. **B784**, 1 (2018), 1708.08692.
- [67] B. I. Abelev et al. (STAR), Phys. Rev. C **79**, 034909 (2009), 0808.2041.
- [68] M. Asakawa and M. Kitazawa, Prog. Part. Nucl. Phys. **90**, 299 (2016), 1512.05038.
- [69] V. Vovchenko and V. Koch, Nucl. Phys. A **1010**, 122179 (2021), 2101.02182.
- [70] M. Gazdzicki, M. I. Gorenstein, M. Mackowiak-Pawlowska, and A. Rustamov, Nucl. Phys. A **1001**, 121915 (2020), 1903.08103.
- [71] This can be confirmed by substituting $(x_1, x_2) = (1, 0)$ and $(y_1, y_2) = (1, 0)$ into Eqs. 14–16

Appendix A: Efficiency correction for higher-order mixed-cumulants

The efficiency correction formulas for higher-order mixed-cumulants are provided in Ref. [56] as

$$\begin{aligned} \langle\langle K_{(x)}^2 K_{(y)} \rangle\rangle_c &= \langle\kappa(1, 0, 1)^2 \kappa(0, 1, 1)\rangle_c + 2\langle\kappa(1, 0, 1)\kappa(1, 1, 1)\rangle_c - 2\langle\kappa(1, 0, 1)\kappa(1, 1, 2)\rangle_c \\ &\quad + \langle\kappa(0, 1, 1)\kappa(2, 0, 1)\rangle_c - \langle\kappa(0, 1, 1)\kappa(2, 0, 2)\rangle_c + \langle\kappa(2, 1, 1)\rangle_c - 3\langle\kappa(2, 1, 2)\rangle_c + 2\langle\kappa(2, 1, 3)\rangle_c, \end{aligned} \quad (\text{A1})$$

$$\begin{aligned}
\langle\langle K_{(x)}^2 K_{(y)}^2 \rangle\rangle_c &= \langle\kappa(1, 0, 1)^2 \kappa(0, 1, 1)^2\rangle_c \\
&+ \langle\kappa(1, 0, 1)^2 \kappa(0, 2, 1)\rangle_c - \langle\kappa(1, 0, 1)^2 \kappa(0, 2, 2)\rangle_c + \langle\kappa(0, 1, 1)^2 \kappa(2, 0, 1)\rangle_c - \langle\kappa(0, 1, 1)^2 \kappa(2, 0, 2)\rangle_c \\
&+ 4\langle\kappa(1, 0, 1) \kappa(0, 1, 1) \kappa(1, 1, 1)\rangle_c - 4\langle\kappa(1, 0, 1) \kappa(0, 1, 1) \kappa(1, 1, 2)\rangle_c \\
&+ 2\langle\kappa(1, 0, 1) \kappa(1, 2, 1)\rangle_c - 6\langle\kappa(1, 0, 1) \kappa(1, 2, 2)\rangle_c + 4\langle\kappa(1, 0, 1) \kappa(1, 2, 3)\rangle_c \\
&+ 2\langle\kappa(0, 1, 1) \kappa(2, 1, 1)\rangle_c - 6\langle\kappa(0, 1, 1) \kappa(2, 1, 2)\rangle_c + 4\langle\kappa(0, 1, 1) \kappa(2, 1, 3)\rangle_c \\
&- 4\langle\kappa(1, 1, 1) \kappa(1, 1, 2)\rangle_c + 2\langle\kappa(1, 1, 1)^2\rangle_c + 2\langle\kappa(1, 1, 2)^2\rangle_c \\
&+ \langle\kappa(2, 0, 1) \kappa(0, 2, 1)\rangle_c - \langle\kappa(2, 0, 1) \kappa(0, 2, 2)\rangle_c - \langle\kappa(2, 0, 2) \kappa(0, 2, 1)\rangle_c + \langle\kappa(2, 0, 2) \kappa(0, 2, 2)\rangle_c \\
&+ \langle\kappa(2, 2, 1)\rangle_c - 7\langle\kappa(2, 2, 2)\rangle_c + 12\langle\kappa(2, 2, 3)\rangle_c - 6\langle\kappa(2, 2, 4)\rangle_c, \tag{A2}
\end{aligned}$$

$$\begin{aligned}
\langle\langle K_{(x)}^3 K_{(y)} \rangle\rangle_c &= \langle\kappa(1, 0, 1)^3 \kappa(0, 1, 1)\rangle_c \\
&+ 3\langle\kappa(1, 0, 1)^2 \kappa(1, 1, 1)\rangle_c - 3\langle\kappa(1, 0, 1)^2 \kappa(1, 1, 2)\rangle_c + 3\langle\kappa(2, 0, 1) \kappa(1, 0, 1) \kappa(0, 1, 1)\rangle_c \\
&- 3\langle\kappa(2, 0, 2) \kappa(1, 0, 1) \kappa(0, 1, 1)\rangle_c + 3\langle\kappa(1, 0, 1) \kappa(2, 1, 1)\rangle_c - 9\langle\kappa(1, 0, 1) \kappa(2, 1, 2)\rangle_c \\
&+ 6\langle\kappa(1, 0, 1) \kappa(2, 1, 3)\rangle_c + 3\langle\kappa(2, 0, 1) \kappa(1, 1, 1)\rangle_c - 3\langle\kappa(2, 0, 1) \kappa(1, 1, 2)\rangle_c - 3\langle\kappa(2, 0, 2) \kappa(1, 1, 1)\rangle_c \\
&+ 3\langle\kappa(2, 0, 2) \kappa(1, 1, 2)\rangle_c + \langle\kappa(3, 0, 1) \kappa(0, 1, 1)\rangle_c - 3\langle\kappa(3, 0, 2) \kappa(0, 1, 1)\rangle_c + 2\langle\kappa(3, 0, 3) \kappa(0, 1, 1)\rangle_c \\
&+ \langle\kappa(3, 1, 1)\rangle_c - 7\langle\kappa(3, 1, 2)\rangle_c + 12\langle\kappa(3, 1, 3)\rangle_c - 6\langle\kappa(3, 1, 4)\rangle_c. \tag{A3}
\end{aligned}$$

One needs to substitute appropriate indices for x and y in Eq. 15 as discussed in Sec. II.